

1        **Supporting Information for “From Stream Flows to**  
2        **Cash Flows: Leveraging Evolutionary Multi-Objective**  
3        **Direct Policy Search to Manage Hydrologic Financial**  
4        **Risk”**

5        **Andrew L. Hamilton<sup>1,2</sup>, Gregory W. Characklis<sup>1,2</sup>, and Patrick M. Reed<sup>3</sup>**

6        <sup>1</sup>Department of Environmental Sciences and Engineering, University of North Carolina at Chapel Hill,  
7        Chapel Hill, North Carolina, USA

8        <sup>2</sup>Center on Financial Risk in Environmental Systems, University of North Carolina at Chapel Hill, Chapel  
9        Hill, North Carolina, USA

10        <sup>3</sup>Department of Civil and Environmental Engineering, Cornell University, Ithaca, New York, USA

11        **Contents of this file**

12        1. Text S1

13        2. Tables S1

14        3. Figures S1-S6

---

Corresponding author: Andrew L. Hamilton, [andrew.hamilton@unc.edu](mailto:andrew.hamilton@unc.edu)

## 15 Introduction

16 This Supporting Information (SI) provides additional methodological details related  
 17 to the power price index (Section S1), in support of Section 2.2 of the main text. Ad-  
 18 ditionally, this SI provides Table S1 (supporting Section 4.2 of the main text), Figure  
 19 S1 (supporting Section 2.1 of the main text), Figure S2 (supporting Section 2.2 of the  
 20 main text), Figure S3 (supporting Section 4.2 of the main text), Figure S4 (supporting  
 21 Section 5.2 of the main text), and Figures S5-S6 (supporting Section 5.3 of the main text).

### 22 S1: Power price index

23 The power price index ( $\varepsilon^P$ , in \$/MWh) is the third stochastic driver described in  
 24 Section 2.2 of the main text. Like the other two drivers,  $\varepsilon^P$  is derived from the one mil-  
 25 lion years of monthly synthetic hydro-financial records from Hamilton, Characklis, and  
 26 Reed (2020); specifically, it is based on the monthly time series of wholesale power price  
 27 and hydropower generation.

28 Let  $\bar{G}_m$  be the average excess hydropower sold into the wholesale market in month  
 29  $m$ . This quantity is highest in the spring and early summer, when the alpine snow melts.  
 30 It is lowest, and negative, during the autumn dry season, when hydropower is often in-  
 31 sufficient to meet retail electricity demand. The generation-weighted-average power price  
 32 for water year  $t$  is defined as

$$33 \quad P_t^{wt} = \frac{1}{12} \frac{\sum_{m=1}^{12} \bar{G}_m P_{m,t}}{\sum_{m=1}^{12} \bar{G}_m} \quad (1)$$

34 where  $P_{m,t}$  is the power price in the  $m$ th month of water year  $t$  (\$/MWh).  $P_t^{wt}$  will be  
 35 highest for years in which dry-season power prices are lower than average and wet-season  
 36 power prices are higher than average, both of which are generally beneficial from a net  
 37 revenue perspective. Now the power price index at the end of water year  $t$  is defined as  
 38 the expected generation-weighted average power price over the coming water year, as pre-  
 39 dicted via linear regression:

$$40 \quad \varepsilon_t^P = \hat{P}_{t+1}^{wt} = \hat{\beta}_0 + \hat{\beta}_1 P_t^{wt} + \hat{\beta}_2 P_{12,t} \quad (2)$$

41 where  $P_{12,t}$  is the power price in September, the final month of the water year, in wa-  
 42 ter year  $t$ , and the  $\hat{\beta}_i$  are estimated regression coefficients. This power price index (in  
 43 units of \$/MWh) is thus the best guess of the generation-weighted-average power price  
 44 over the coming water year,  $t+1$ , using the information available from the current wa-

45 ter year,  $t$ . This index takes advantage of the autocorrelation in wholesale power prices  
 46 to predict whether the prices over the coming water year will be more or less beneficial  
 47 for net revenues. For this reason, it is potentially valuable information for making de-  
 48 cisions regarding financial risk, and is used as one of the informational inputs to the dy-  
 49 namic control policies, as discussed in Section 3.1.2 of the main text.

## 50 Tables

**Table S1.** Parameters for multi-objective optimization with the Borg Multi-Objective Evolutionary Algorithm.

Parameter	Value
Number of samples per function evaluation	50,000
Number of function evaluations per Borg MOEA run	150,000
Number of seeds for Borg MOEA	30
Number of radial basis functions ( $M$ )	2
Number of informational inputs to policy ( $L$ )	4
$\epsilon$ -dominance parameter for $J^{cash}$	\$0.075 M/year
$\epsilon$ -dominance parameters for $J^{debt}$	\$0.225 M
$\epsilon$ -dominance parameter for $J^{hedge}$	\$0.05001
$\epsilon$ -dominance parameters for $J^{fund}$	\$0.225 M

51 **Figures**

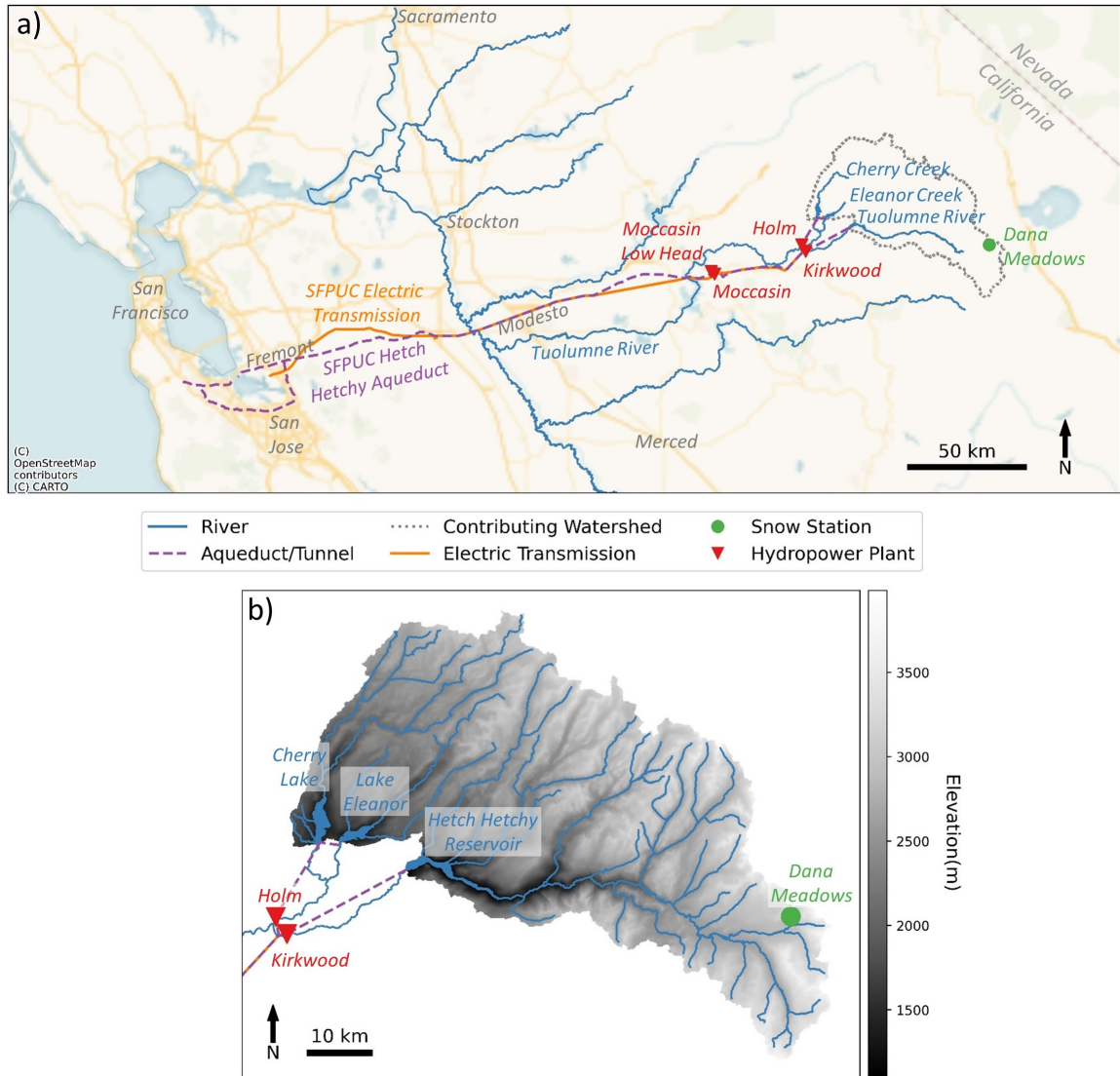


**Figure S1.** (a) Map of the study region. (b) Zoomed in map of the contributing watershed.

Figure reproduced from Hamilton et al. (2020) Supporting Information.

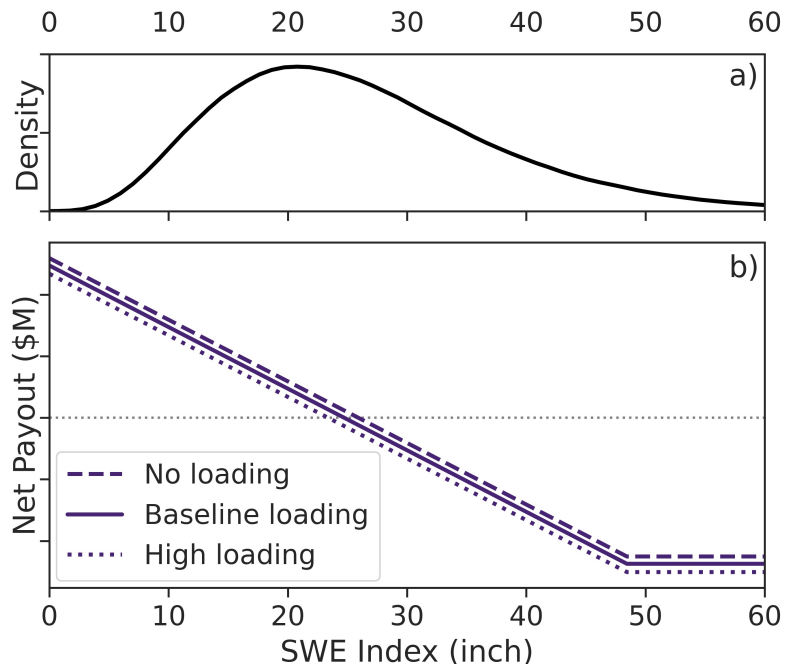


**Figure S2.** (a) Probability density for SWE index, a weighted average of February 1 and April 1 observations. (b) Net payout function for the capped contract for differences (CFD). The threshold separating positive and negative payouts is 24.71 inches. The slope of this contract is controlled by either the static or dynamic control policy. Present study uses the “baseline” loading. Figure adapted from Hamilton et al. (2020).

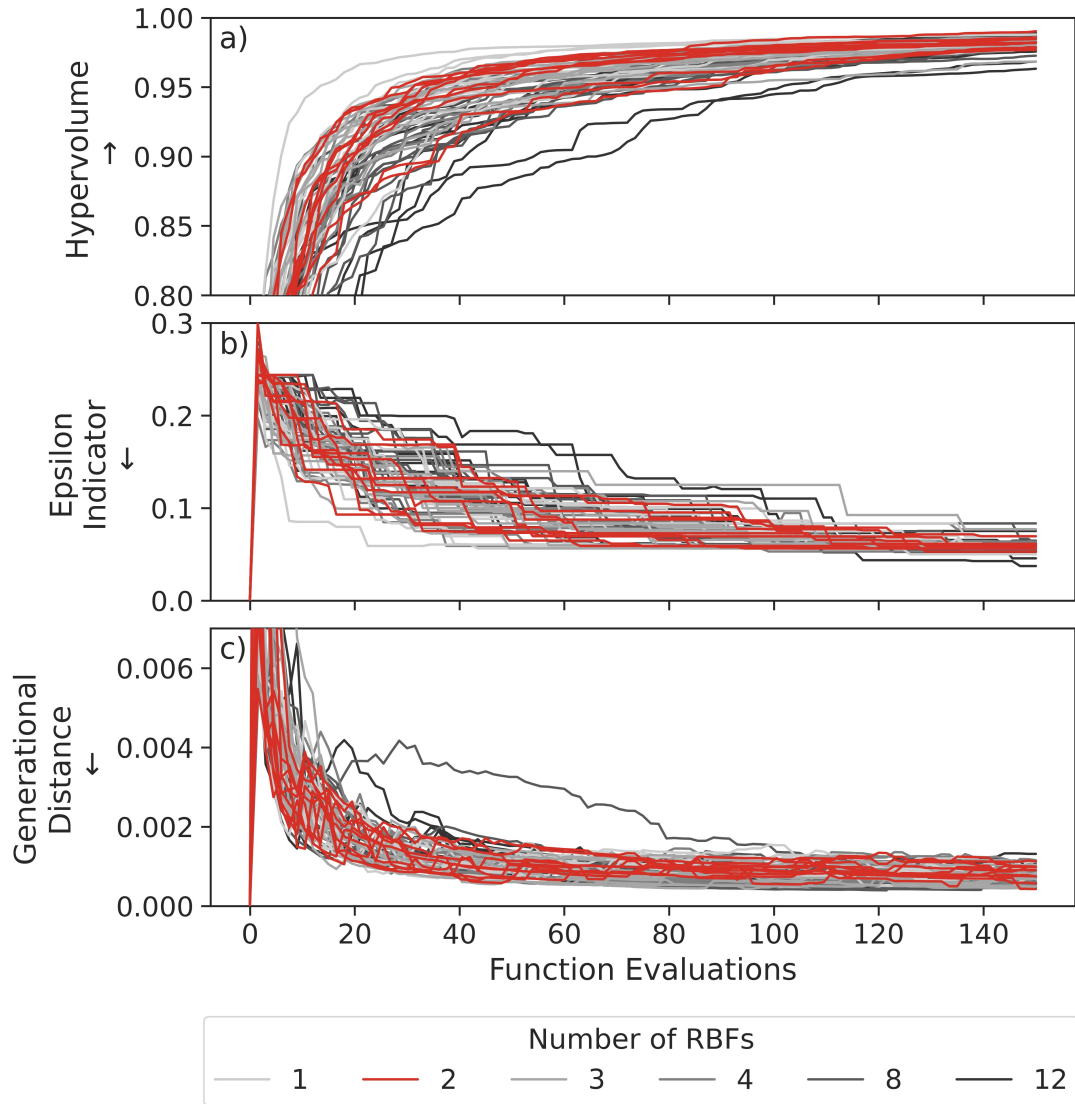


**Figure S3.** Convergence metrics for approximate Pareto sets from the Borg MOEA, using different numbers of radial basis functions (RBFs), for 10 random seeds each: (a) Hypervolume metric; (b) Generational distance metric; (c) Additive epsilon indicator metric.

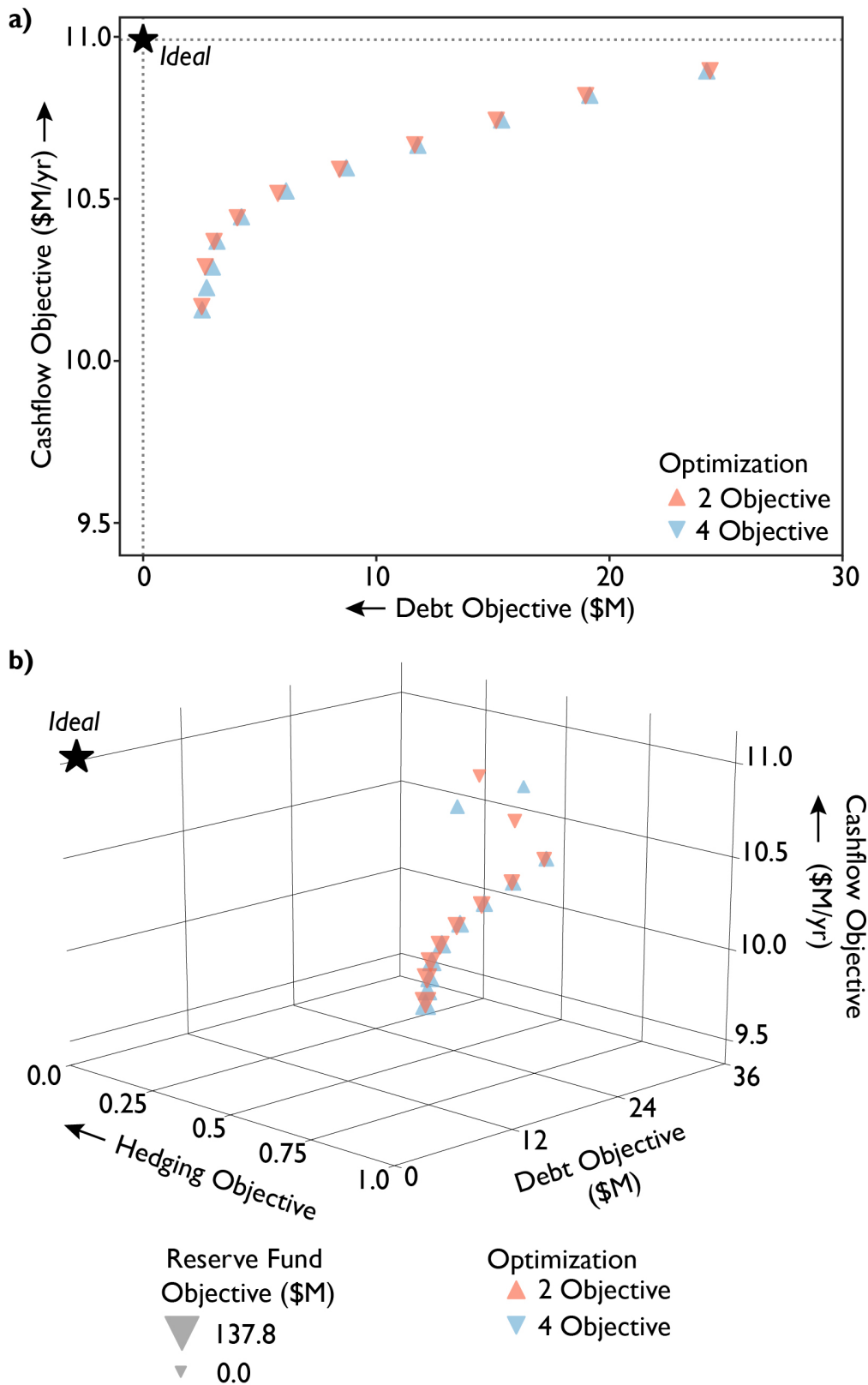


**Figure S4.** Results from 2-objective and 4-objective optimization problems, after filtering for non-dominated solutions with respect to the 2-objective problem ( $J^{cash}$  vs.  $J^{debt}$ ). Results displayed for both 2-objective (a) and 4-objective (b) performance.

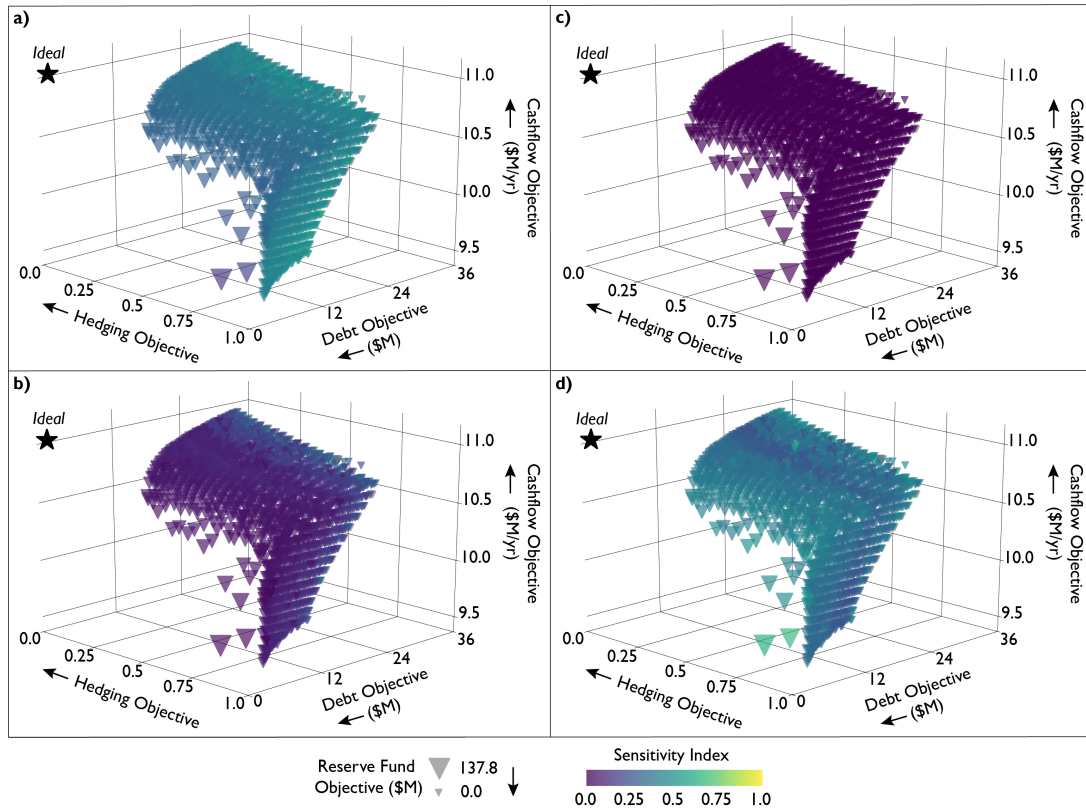


**Figure S5.** Entropic sensitivity indices, relative to withdrawal/deposit decision, for the reserve fund balance (a), debt (b), power price index (c), and incoming cash flow (Cash Flow 2) (d).

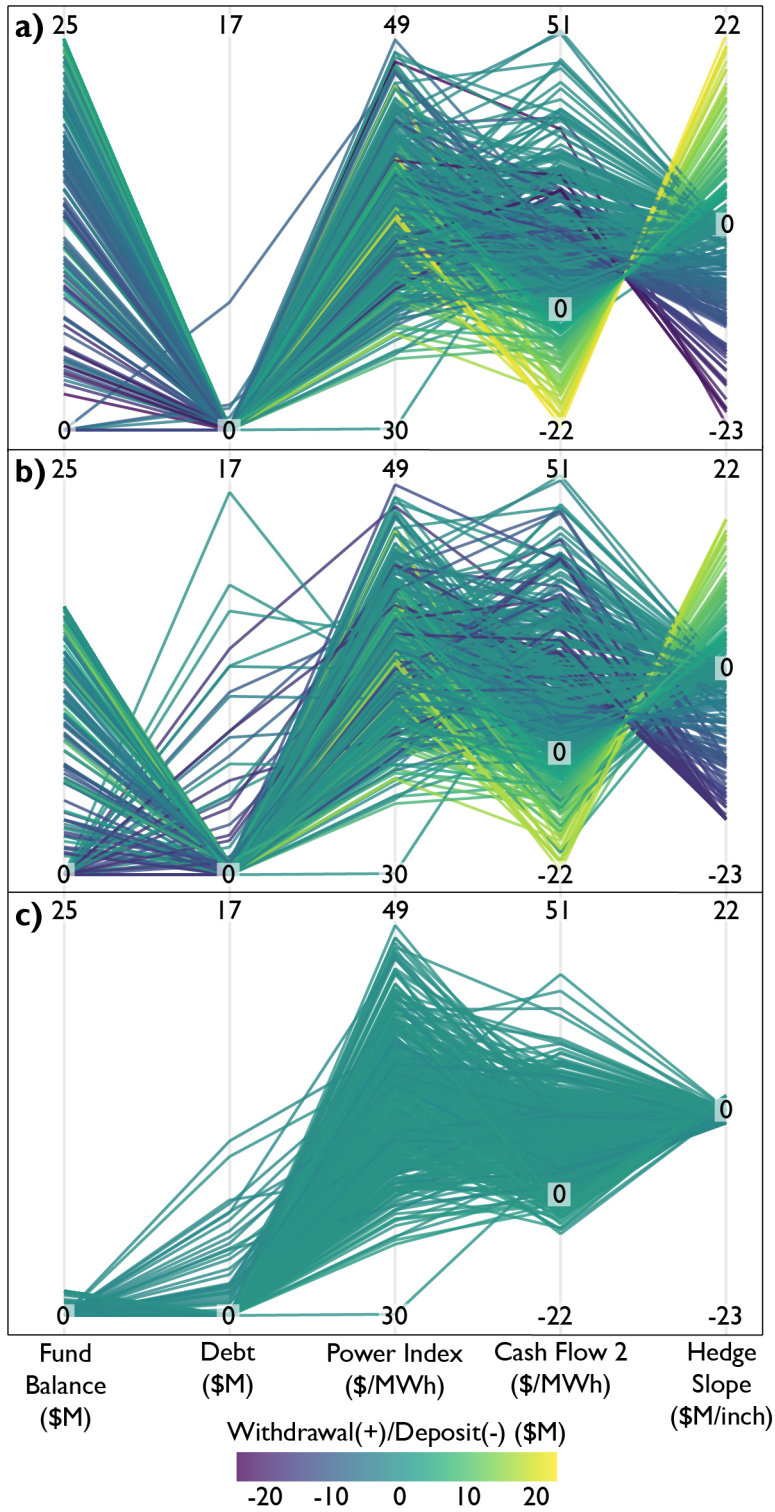


**Figure S6.** Withdrawal/Deposit control policy visualization for three chosen policies in Figure 8 and rows 4-6 of Table 2 in the main text. The policies are chosen due to their high sensitivity (with respect to the hedging control policy) to the reserve fund (a), debt (b), and power price index (c) information.

52 **References**

- 53 Hamilton, A. L., Characklis, G. W., & Reed, P. M. (2020). Managing financial risk  
54 tradeoffs for hydropower generation using snowpack-based index contracts.  
55 *Water Resources Research*, 56, e2020WR027212. doi: 10.1029/2020wr027212